Ferroelectricity in an $S = 1/2$ Chain Cuprate

S. Park, Y. J. Choi, C. L. Zhang, and S-W. Cheong

Rutgers Center for Emergent Materials & Department of Physics and Astronomy, Rutgers University, Piscataway, New Jersey 08854, USA

(Received 19 September 2006; published 31 January 2007)

We report our discovery of ferroelectricity in the spiral-magnetic state in the quantum quasi-one-dimensional (1D) $S = 1/2$ magnet of $LiCu_2O_2$. Electric polarization (P) emerges along the c direction below the spiral-magnetic order temperature, but changes from the c to a axis when magnetic fields (H) are applied along the b direction. We also found that P_c increases with H_c, and P_a appears with H_a. $LiCu_2O_2$ in zero field appears to be the first ferroelectric cuprate and also a prototypical example of the "1D spiral-magnetic ferroelectrics." However, the unexpected behavior in H may demonstrate the complexity of the ordered spin configuration, inherent in the 1D $S = 1/2$ magnet of $LiCu_2O_2$.

DOI: 10.1103/PhysRevLett.98.057601 PACS numbers: 77.80.Fm, 75.10.Pq, 75.80.+q, 77.22.Ej

Ferroelectricity is the electronic version of magnetism, associated with the polar arrangement of charges. Ferroelectricity turns out to be mutually exclusive to magnetism because, for example, in the class of transition metal oxides, to which most ferroelectrics belong, the nonzero d electrons, required for the presence of magnetic moments, tend to reduce the energy gain associated with ferroelectric distortion [1,2]. Therefore, only a limited number of compounds, the so-called multiferroics, exhibit the coexistence of magnetism and ferroelectricity. Even in the multiferroics, the interaction between magnetism and ferroelectricity is rather weak. Recent discoveries of spectacular cross-coupling effects in frustrated magnets, such as reversibly flipping ferroelectric polarization or a drastic change of the dielectric constant with applied magnetic fields, offer new opportunities for a thorough scientific understanding of multiferroicity as well as multiferroic applications [3–7].

Multiferroics with enhanced cross-coupling effects exhibit magnetic orders with broken centrosymmetry. It turns out that the lattice relaxation through exchange striction associated with the magnetic orders with noncentrosymmetry is the origin of magnetism-induced ferroelectricity [8–11]. The exchange coupling between spins, where exchange striction is associated, is a tensorial quantity, and has symmetric parts and antisymmetric parts. The symmetric parts seem to be relevant to multiferroicity in systems such as RMn_2O_5 [12], and the antisymmetric parts, which constitute the so-called Dzyaloshinskii-Moriya (DM) interaction, become active when ferroelectricity is induced by spiral-magnetic orders in systems such as $TbMnO_3$, $Ni_3V_2O_8$, delafossite $CuFeO_2$, hexaferrite $(Ba, Sr)_2Zn_2Fe_{12}O_{22}$, spinel $CoCr_2O_4$, and $MnWO_4$ [13–19]. Note that $TbMnO_3$, $CoCr_2O_4$, and $MnWO_4$ are 3D compounds, and $Ni_3V_2O_8$ and $CuFeO_2$ are quasi-2D systems.

A prototypical condition for obtaining a spiral-magnetic order is when in a chain magnet the nearest-neighbor (NN) ferromagnetic coupling (J_F) competes with the next-nearest-neighbor (NNN) antiferromagnetic coupling (J_{AF}). In a classical regime, it is well known that when $|J_{AF}/J_F|$ is larger than $1/4$, a spiral order with $2\pi\xi = \cos^{-1}(1/|4J_{AF}/J_F|)$ (pitching angle $= 2\pi\xi$) becomes the ground state [20]. Even though it has been controversial, $LiCu_2O_2$ appears to be a wonderful example of this 1D spiral magnet with NN $J_F \approx -11 \pm 3$ meV and NNN $J_{AF} \approx +7 \pm 1$ meV [21–24]. In $LiCu_2O_2$, 4 planar oxygens among five oxygens coordinating a Cu^{2+} ion form an edge sharing plate extending to the chain b direction, and lead to a $\sim 94°$ NN superexchange route along the b axis as shown in Fig. 1(a). The presence of the magnetic superlattice peak of (0.5, 0.826, 0) was reported, and thus the spiral modulation ξ along the chain direction is 0.174, which corresponds to the pitching angle of 62.6° [21]. These experimental values are in accordance with the estimated ratio of $|J_{AF}/J_F| \approx 0.50$–$0.65$. From neutron scattering results, it was proposed that the spiral plane is the ab plane [21]. However, our experimental results seem to be inconsistent with the proposition of the ab spiral plane.

Herein, we report our surprising discovery that the quantum $S = 1/2$ chain magnet of $LiCu_2O_2$ exhibits ferroelectricity when the spiral-magnetic order sets in.

Single crystals of $LiCu_2O_2$ were grown by the self-flux method using excessive CuO_2 powders as a flux in a Pt crucible. Black platelet crystals with the size of ~ 0.2 cm^3 were obtained after slowly cooling from 1250 to 950 °C in air. X-ray powder diffraction results at room temperature indicated a single phase of $LiCu_2O_2$ with an orthorhombic unit cell [$Pnma$, $a = 5.734(4)$ Å, $b = 2.856(2)$ Å, and $c = 12.415(6)$ Å]. Insulating pieces were collected and cut in a rectangular shape with a cross sectional area of 3–4 mm^2 and a thickness of 0.2–0.4 mm. The resistances of the specimens are $\sim 10^7$ Ω at room temperature and too large to be measured below ~ 150 K. The dielectric constant (ε) was measured by an LCR meter at $f = 28$ kHz with an excitation of 1 V. Pyroelectric and magnetoelectric currents were measured with an electrometer at a rate of 4 K/s and 0.02 T/s, respectively, after cooling specimens in a static poling electric field of $E_{pole} = 400$–1200 kV/m

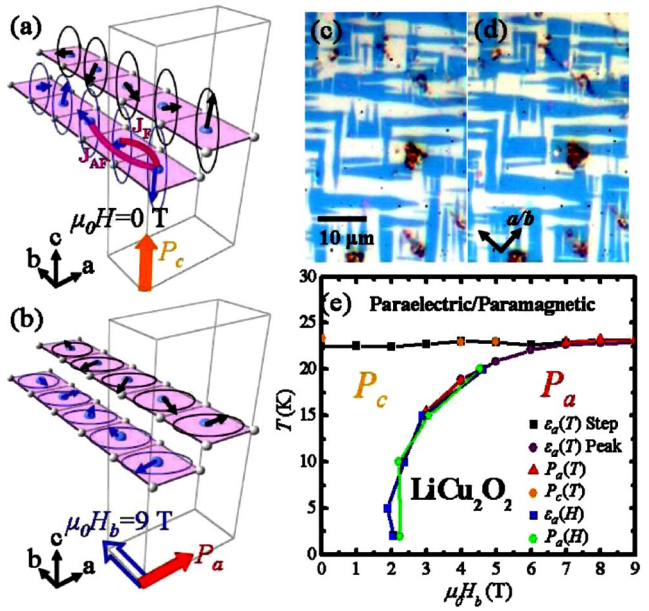

FIG. 1 (color online). (a) Proposed spiral spin structure in zero field, consistent with the presence of a finite electric polarization (P) along the c axis. Cu^{2+} ions (in blue or medium gray) are coordinated by five oxygen atoms (in white) including one apical one. (b) Proposed spiral spin structure in $H = 9$ T along the b axis. In H_b, P switches to the a axis. (c),(d) Polarized optical microscope images of the ab plane of $LiCu_2O_2$. The domain boundaries appear with 45° away from the crystallographic a/b axes (in arrows). (e) Phase diagram of $LiCu_2O_2$, showing the presence of a paraelectric–paramagnetic state, a FE state with P_c and a FE state with P_a induced by H_b.

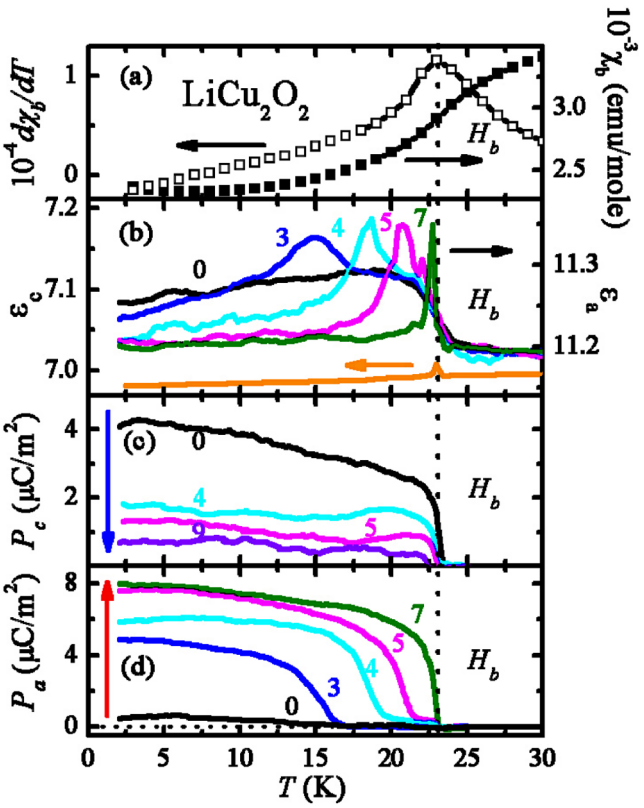

FIG. 2 (color online). (a) Magnetic susceptibility (χ) and $d\chi/dT$ in $H_b = 2$ kOe vs temperature. (b) Dielectric constants (ε) along the a and c axes. H_b dependence of ε_a is also shown. (c) Temperature dependence of P_c in H_b. All experiments for the H_b dependence were performed in field cooling. (d) Temperature dependence of P_a in H_b.

(the poling field was removed just before the measurements). A SQUID magnetometer was used for magnetization measurement.

A twin structure was observed in the ab plane of the $LiCu_2O_2$ crystal under a polarized optical microscope (POM), as shown in Figs. 1(c) and 1(d). Contrast under POM reverses by slightly changing the angle between a polarizer and an analyzer around 90°, confirming that the contrast originates from ~90° twins. The twin structure exists because of the similarity in magnitude between the a lattice constant and twice of the b lattice constant [25]. Note that for our macroscopic-size specimens with microscopic twins, we will use the notation of a and b in the way consistent with the concept of spiral-magnetic ferroelectricity. The electric polarization (P) and ε along the twinned a/b direction are denoted as P_a and ε_a, respectively. When H is applied perpendicular to the electric field for ε and P measurements in the ab plane, it is denoted as H_b. When applied parallel, it is denoted as H_a. These notations are used because within the framework of spiral-magnetic ferroelectricity, P is supposedly perpendicular to the spin chain direction, i.e., the b direction. Figure 2(a) shows the temperature (T) dependence of the magnetic susceptibility (χ) and its temperature derivative along the a/b axis. A broad hump of χ (T) at ~40 K is attributed to the formation of short-range magnetic correlations in the 1D $S = 1/2$ system, and the weak but sharp features in $\chi(T)$ and $d\chi(T)/dT$ at $T_N = 23$ K signify the onset of an antiferromagnetic (AFM) long-range ordering [26]. The T dependence of ε along both the a and c directions is displayed in Fig. 2(b). ε along the c axis, ε_c, reveals a tiny but sharp peak at 23 K, which coincides well with T_N, indicated in $\chi(T)$. Along the a axis, a relatively large steplike increase of ε, however, appears below T_N. With applied magnetic fields along the b axis (H_b), $\varepsilon_a(T)$ in $H_b = 3$ T shows a broad peak at ~15 K, which approaches to T_N in higher H_b, while the steplike anomaly at T_N persists for H_b up to 5 T.

These ε features below T_N stem from the emergence of electric polarization in the magnetically ordered state in $LiCu_2O_2$. Figures 2(c) and 2(d) exhibit the T dependence of polarization along the c (P_c) and the a (P_a) axes in H_b, measured upon warming after removing E_{pole} at 2 K. First of all, P_c becomes nonzero below T_N, consistent with the presence of a sharp ε_c peak at T_N. This polarization is found to reverse when a negative E_{pole} was applied. These behaviors clearly indicate that a ferroelectric state emerges when a magnetic order sets in. With applied H_b, P_c decreases, and becomes negligible in $H_b = 9$ T. On the other

hand, P_a seems to be absent in $H = 0$ T, but appears in $H_b = 3$ T below ~15 K. The transition T for P_a moves slowly up to ~23 K with increasing $H_b > 3$ T.

This change of the transition T of P_a in H_b is consistent with the behavior of the broad ε_a peak in H_b, shown in Fig. 2(b). However, this P_a behavior in H_b is seemingly different from that of P_c, showing a single transition T in various H_b. This is unusual if the appearance of P_a results from the suppression of P_c with increasing H_b. To unveil the origin of this different behavior, we measured the pyroelectric current for P_c in H_b in different ways. For example, the specimen was cooled in a constant E_{pole} to 20 K in 3 T, and the E_{pole} was removed afterwards. Pyroelectric current for P_c was, then, measured while cooling the specimen in 3 T from 20 K to 2 K, and this pyroelectric current shows a distinct feature at 15 K, which appears in a way consistent with the suppression of P_c below 15 K. This observation indicates that the absence of the low-T transition (such as the 15 K transition in 3 T) in $P_c(T)$ in H_b in Fig. 2(c) is due to the loss of poling information below the low-T transition, i.e., the appearance of ferroelectric domains when E_{pole} was removed at 2 K.

The H_b dependence of P_c, P_a, ε_a, and M/H at 10 and 20 K, shown in Fig. 3, clearly demonstrates that H_b induces the flipping of P from the c to a direction. While P_c in Fig. 3(a) shows the decrease of its magnitude with increasing H_b, P_a in Fig. 3(b) exhibits an opposite behavior. The corresponding threshold fields are the same for both $P_c(H_b)$ and $P_a(H_b)$, and this transition is also evident in $\varepsilon_a(H_b)$ at 10 K shown in Fig. 3(c). This field induced transition occurs at a higher H_b at 20 K, as apparent in $P_a(H_b)$ in Fig. 3(b) and in $\varepsilon_a(H_b)$ in Fig. 3(c). Figure 3(b) also demonstrates that repeatedly reversing H_b induces the suppression of P_a upon the magnetic field cycling. This suppression possibly originates from the induction of ferroelectric multidomains when polarization flipping occurs. Figure 3(d) indicates that the small kinks in $H_b \approx 2.4$ T (at 10 K) and ≈ 4.5 T (at 20 K) in $M/H(H_b)$ match with the transitions indicated in $P_c(H_b)$, $P_a(H_b)$, and $\varepsilon_a(H_b)$. Both the reversible behavior of the polarization in opposite E_{pole} and the presence of the magnetization anomalies at the consistent threshold H fields support that the polarization results from a bulk effect. For the T and H_b dependence of ε_a and P_a, we have constructed a magneto-electric phase diagram of $LiCu_2O_2$ for H_b, as displayed in Fig. 1(e). The low-H_b state below $T_N \approx 23$ K is a ferroelectric magnetic state with a finite P_c, and high H_b induces the flip of the electric polarization direction from the c to a axis.

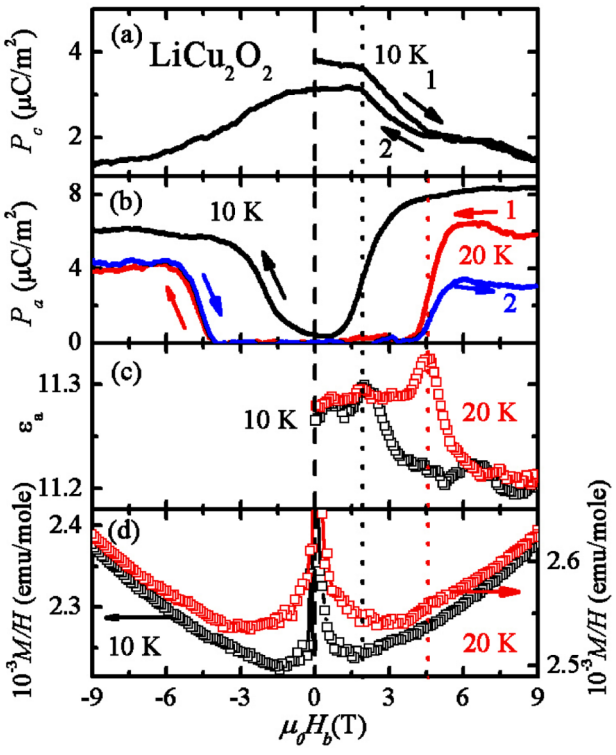

FIG. 3 (color online). H_b dependence of (a) P_c at 10 K and (b) P_a at 10 K and 20 K. H_b reverse-cycling at 20 K shows the reduction of P_a. H_b dependence of (c) ε_a and (d) M/H at 10 K and 20 K. The H_b-induced transitions of ε at both temperatures are consistent with those of polarizations.

In spiral magnets, the DM interaction induces the magnetically driven polarization proportional to $\mathbf{e}_{ij} \times (\mathbf{S}_i \times \mathbf{S}_j)$, where $\mathbf{e}_{ij}$ is the vector connecting the two $\mathbf{S}_i$ and $\mathbf{S}_j$ spins [8]. Our observation of a finite P_c in zero H, combined with the concept of spiral-magnetic ferroelectricity and earlier report of $\mathbf{Q} = (0.5, 1 - \xi, 0)$ with the spin chain along the b axis, indicates that the spiral spins, relevant to the finite P_c, lie on the bc plane; i.e., $\mathbf{S}_i \times \mathbf{S}_j$ is along the a axis. When a magnetic field applied along the b axis, P_c decreases and P_a increases, implying that the Cu^{2+} spin spiral plane flips from the bc to ab plane, resulting the flip of the polarization from the c to a axis as depicted in Figs. 1(a) and 1(b). Note that this picture may be simplified, and represents a projection of the actual configuration of complex spiral spins that is relevant to the presence of the electric polarization [27].

Figure 4(a) shows the T dependence of ε along the a axis (ε_a) in magnetic fields along the same a axis (H_a): note that the polarization and dielectric constant along the twinned a/b direction are denoted as P_a and ε_a as discussed earlier. Unexpectedly, ε_a decreases with increasing H_a and a small peak appears at $H_a = 9$ T at 22.2 K, which is slightly lower than $T_N \approx 23$ K. Accordingly, P_a appears and then increases with increasing H_a as shown in Fig. 4(b). Furthermore, as depicted in Fig. 4(b), P_c also increases as H_c increases. The H_a dependent of ε_a and P_a is displayed Fig. 4(e), showing the smooth increase of P_a with increasing H_a at 10 K and 20 K without phase transitionlike features.

In general, spins without a net moment (such as antiferromagnetic or spiral spins) tend to orient perpendicular to an applied magnetic field [10]. Thus, it is expected that H_c may flip the spiral plane from the bc to ab plane, so that P may flip from the c to a axis with H_c. However, this is

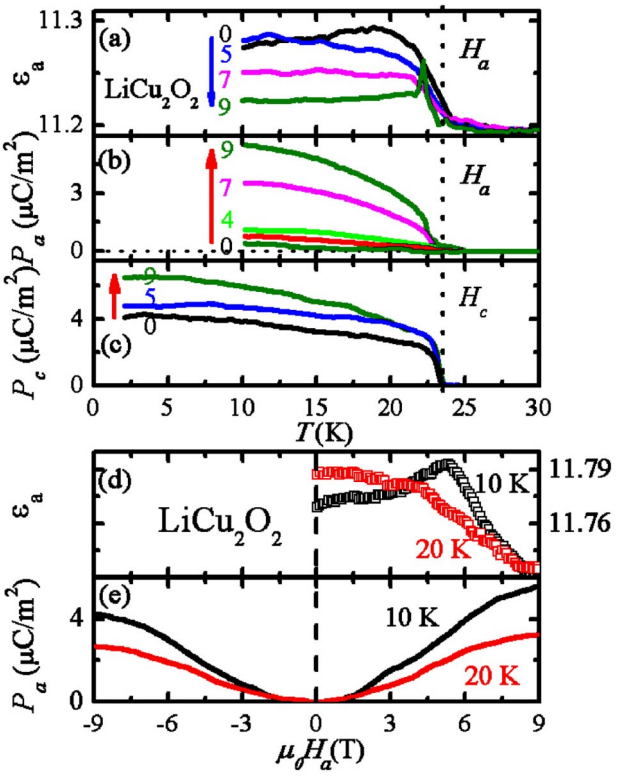

FIG. 4 (color online). (a) Temperature dependence of ε_a with H_a. (b) P_a with H_a. (c) $P_c$with H_c. (d) H_a dependence of ε_a at 10 K and 20 K. (e) H_a dependence of P_a at 10 K and 20 K, exhibiting a smooth change of polarization with increasing H_a.

completely in contrast with our observation: H_c enhances P_c and H_b is the one inducing the P flip from the c to a axis. The appearance of P_a with H_a is also counterintuitive within the framework of spiral-magnetic ferroelectricity. These unexpected magnetic field effects may stem from the complexity of the spiral-magnetic order in the 1D $S = 1/2$ magnet. Note that a strong competition between quantum spin fluctuations and the incommensurate helimagnetic state was reported [21]. We also point out that from NMR experiment, Gippius *et al.* suggested that spins rotate on the plane containing the chain while also precessing around the chain [27]. This complex spin configuration may be associated with the quantum and fluctuating nature of $LiCu_2O_2$, and the details of this intriguing magnetism remain to be explored. Nevertheless, the behavior of the electric polarization in $H = 0$ can be understood in a simple model based on the framework of spiral-magnetic ferroelectricity as discussed above. We emphasize that as observed in other spiral-magnetic ferroelectrics, the electric polarization is weak, and the appearance of this weak polarization is closely connected to the long-range magnetic ordering. It is evident that the magnitude of ξ is directly related with the ratio of $|J_{AF}/J_F|$, and an applied magnetic field is expected to be of assistance to J_F, so that the magnitude of ξ can be readily modified with magnetic fields [28,29]. The magnetically driven polarization is proportional to $\mathbf{e}_{ij} \times (\mathbf{S}_i \times \mathbf{S}_j)$, where $\mathbf{S}_i \times \mathbf{S}_j$ gives the connection to the pitching angle [8]. Therefore, the change of the spiral modulation wave length, inversely proportional to the pitching angle, should affect the magnitude of the electric polarization.

In summary, we have discovered the emergence of a ferroelectric polarization in the spiral-magnetic state in the 1D $S = 1/2$ cuprate of $LiCu_2O_2$ where spiral-magnetic order originates from the competition between NN ferromagnetic and NNN antiferromagnetic couplings. Thus, $LiCu_2O_2$ is the first example of a ferroelectric cuprate (as far as we are aware of), and appears to be a prototypical example of 1D spiral-magnetic ferroelectrics. Applying magnetic fields can significantly influence the ferroelectric polarization as well as dielectric constants. Understanding the origin of these remarkable magnetic field effects requires further studies on this fascinating ferroelectric cuprate.

We thank L. Mihály and M. Mostovoy for useful discussions. This work was supported by NSF-DMR-0520471.

[1] N. A. Hill, J. Phys. Chem. B **104**, 6694 (2000).
[2] D. I. Khomskii, J. Magn. Magn. Mater. **306**, 1 (2006).
[3] T. Kimura *et al.*, Nature (London) **426**, 55 (2003).
[4] T. Goto *et al.*, Phys. Rev. Lett. **92**, 257201 (2004).
[5] N. Hur *et al.*, Nature (London) **429**, 392 (2004).
[6] N. Hur *et al.*, Phys. Rev. Lett. **93**, 107207 (2004).
[7] B. Lorenz *et al.*, Phys. Rev. Lett. **92**, 087204 (2004).
[8] H. Katsura, N. Nagaosa, and A. V. Balatsky, Phys. Rev. Lett. **95**, 057205 (2005).
[9] I. A. Sergienko, and E. Dagotto, Phys. Rev. B **73**, 094434 (2006).
[10] Maxim Mostovoy, Phys. Rev. Lett. **96**, 067601 (2006).
[11] A. B. Harris *et al.*, Phys. Rev. B **73**, 184433 (2006).
[12] L. C. Chapon *et al.*, Phys. Rev. Lett. **96**, 097601 (2006).
[13] T. Arima *et al.*, Phys. Rev. Lett. **96**, 097202 (2006).
[14] M. Kenzelmann *et al.*, Phys. Rev. Lett. **95**, 087206 (2005).
[15] G. Lawes *et al.*, Phys. Rev. Lett. **95**, 087205 (2005).
[16] T. Kimura, J. C. Lashley, and A. P. Ramirez, Phys. Rev. B **73**, 220401(R) (2006).
[17] T. Kimura, G. Lawes, and A. P. Ramirez, Phys. Rev. Lett. **94**, 137201 (2005).
[18] Y. Yamasaki *et al.*, Phys. Rev. Lett. **96**, 207204 (2006).
[19] K. Taniguchi *et al.*, Phys. Rev. Lett. **97**, 097203 (2006).
[20] R. Bursill *et al.*, J. Phys. Condens. Matter **7**, 8605 (1995).
[21] T. Masuda *et al.*, Phys. Rev. Lett. **92**, 177201 (2004); T. Masuda *et al.*, Phys. Rev. B **72**, 014405 (2005).
[22] A. A. Gippius *et al.*, Phys. Rev. B **70**, 020406(R) (2004); S.-L. Drechsler *et al.*, Phys. Rev. Lett. **94**, 039705 (2005).
[23] M. Papagno *et al.*, Phys. Rev. B **73**, 115120 (2006).
[24] L. Mihály *et al.*, Phys. Rev. Lett. **97**, 067206 (2006).
[25] R. Berger, P. Önnerud, and R. Tellgren, J. Alloys Compd. **184**, 315 (1992).
[26] Our susceptibility data up to room temperature are basically identical with the published result in Ref. [21].
[27] A. A. Gippius *et al.*, J. Magn. Magn. Mater. **300**, e335 (2006).
[28] V. Kiryukhin, B. Keimer, and D. E. Moncton, Phys. Rev. Lett. **74**, 1669 (1995).
[29] A. Zheludev *et al.*, Phys. Rev. Lett. **78**, 4857 (1997).